arXiv:cond-mat/0702332v1 [cond-mat.mes-hall] 14 Feb 2007

Shot Noise with Interaction Effects in Single Walled Carbon Nanotubes

F. Wu[1], P. Queipo[2], T. Tsuneta[1], T. H. Wang[3], E. Kauppinen[2] and P. J. Hakonen[1]
[1]*Low Temperature Laboratory, Helsinki University of Technology, Espoo, Finland*
[2]*Center for New Materials, Helsinki University of Technology, Espoo, Finland*
[3]*Chinese Academy of Sciences, Beijing, China*
(Dated: February 6, 2008)

We have measured shot noise in single walled carbon nanotubes (SWNT) with good contacts at 4.2 K at low frequencies ($f = 600 - 850$ MHz). We find a strong modulation of shot noise over the Fabry-Perot pattern; in terms of differential Fano factor the variation ranges over 0.4 - 1.2. The shot noise variation, in combination with differential conductance, is analyzed using two (spin-degenerate) modes with different, energy-dependent transmission coefficients. No power law dependence of shot noise, as expected for Luttinger liquids, was found in our measurements.

Shot noise measurements have proven to be useful in providing information on the fundamental conduction mechanisms in mesoscopic conductors [1]. For example, shot noise has been utilized to determine the effective charge of quasiparticles in fractional quantum Hall systems [2, 3]. In multiterminal conductors, current-current cross-correlations have been employed for investigating the fermionic nature of charge carriers [4, 5]. Also in single walled carbon nanotubes (SWNT), noise is expected to be a valuable tool for studying the physics of charged elementary excitations [6, 7, 8, 9, 10, 11, 12, 13].

Liang et al. in Ref. 14 have shown that SWNTs may act as molecular waveguides for electronic transport. They employed a scattering matrix approach to show that the results could be understood in terms of Fabry-Perot type of interference in which reflection at the contacts played a crucial role [14, 15]. Shot noise in the Fabry-Perot regime was recently studied at 4.2 K by Kim et al. [12] who found power law dependence at low bias voltages as well as oscillations as a function of bias voltage. These findings were assigned to Luttinger liquid behavior of SWNTs.

We have measured shot noise and AC conductance in a SWNT sample which displays a rather asymmetric Fabry-Perot resonance pattern. The interference pattern has a strong modulation, mostly dominated by a single mode: the contribution from the second is only about $0.1 \cdot 2e^2/h$. We find a strong modulation of noise over the Fabry-Perot pattern which we characterize in terms of a differential Fano-factor F_d. The resonance condition is reflected as a strong suppression of shot noise with $F_d \simeq 0.4$ while the destructive interference yields $F_d \simeq 1.2$. We model our result successfully using regular quantum conductor formalism with energy-dependent transmission coefficients, without any recourse to Luttinger liquid (LL) physics.

The current in a quantum dot can be expressed in terms of energy ϵ dependent transmission coefficient $I = \frac{2e}{h}\int_0^{eV}\sum_{i=1}^{N}\tau_i(\epsilon,V)d\epsilon$, where $\tau_i(\epsilon,V)$ denotes the transmission coefficient of spin-degenerate mode i and we assume that the voltage is applied to one terminal only. For differential conductance G_d, this yields

$$G_d = \frac{dI}{dV} = \frac{d}{dV}\left(\frac{2e}{h}\int_0^{eV}\sum_{i=1}^{N}\tau_i(\epsilon,V)d\epsilon\right). \qquad (1)$$

In the case of non-interacting electrons, $\tau(\epsilon,V)$ is voltage independent and Eq. (1) reduces to $dI/dV = G_0\sum_{i=1}^{N}\tau_i(eV)$ with $G_0 = 2e^2/h$.

The low-frequency shot noise is given by

$$\underline{\mathrm{S}}(V) = \int dt\langle\delta I(t)\delta I(0) + \delta I(0)\delta I(t)\rangle \qquad (2)$$
$$= \frac{4e^2}{h}\int_0^{eV}\sum_{i=1}^{N}\tau_i(\epsilon)\left(1-\tau_i(\epsilon)\right)d\epsilon,$$

where $\delta I(t) = I(t) - \langle I(t)\rangle$ at voltage V, and the current-current correlator reduces to the latter form in the absence of interactions. By combining Eqs. (1) and (2) we may define the differential Fano-factor as

$$F_d = \frac{1}{2e}\frac{dS}{dV}\Big/\frac{dI}{dV} = \frac{1}{2e}\frac{dS}{dI}. \qquad (3)$$

This is a quantity that we probe in our sensitive noise measurements based on lock-in detection on modulated noise signal.

In the above formulas, it is assumed that $eV \gg k_BT$. In the cross-over regime with $eV \sim k_BT$, one may write for the excess noise, the difference of current noise and thermal noise

$$S(I) - S(0) = \frac{4k_BT}{R(0)}\left(KF\frac{eV}{2k_BT}\coth\left(\frac{eV}{2k_BT}\right) - 1\right), \qquad (4)$$

where $S(0)$ specifies the noise at zero bias, $R(0) = V/I$ in the limit $V \to 0$, $K = 1$ and F denotes the Fano-factor. Formally, the left side can be identified as $\int_0^I \frac{dS}{dI}dI = \int_0^I 2eF_d dI$. Hence, Eq. (4) provides an interpolation formula for the average Fano factor $\widetilde{F} = \frac{1}{I}\int_0^I F_d dI$ that is obtained from our measurements. Note that

$\widetilde{F} = (S(I) - S(0))/(2eI)$ is the quantity that is often used to determine the Fano-factor [16]; at large $V \gg k_B T/e$, $\widetilde{F}$ is equivalent to F in Eq. (4). Finally, in order to take into account non-linearities of IV-curve we set $K = R(0)/(I/V)$ in Eq. (4).

In the nonlinear regime, noise measurements are sensitive to changes in the sample resistance. For our setup, where a sample having a dynamic resistance of R_d is connected directly to a preamplifier with impedance $R_L = 50$ Ω, we may derive the following equation (using the equivalent circuit displayed in the inset of Fig. 2)

$$\frac{1}{G_{cal}} \frac{1}{R_L} \frac{\Delta P}{\Delta I} = 2eF_d - 2eF_d \frac{2R_L}{R_d} - 2i_n^2 R_d R_L \frac{\partial^2 I}{\partial V^2}, \quad (5)$$

which relates the measured, gain-adjusted noise power variation $\frac{1}{G_{cal}} \frac{\Delta P}{\Delta I}$ to F_d ($= \frac{1}{2e} \frac{dS}{dV} / \frac{dI}{dV}$). The second term on the right describes the first order correction in measured shot noise due to changes in R_d while the third term takes into account corrections caused by the total system noise due to non-linearities, *i.e.* i_n^2 marks the full noise at the operating point, including the preamplifier noise. The calibration constant G_{cal} remains fixed within the factor $1 + \frac{2R_L}{R_T} - \frac{2R_L}{R_d}$, where R_T denotes the resistance of the tunnel junction employed in the calibration. In the data analysis, we neglect the corrections due to small changes in G_{cal} as well as the term $2e\frac{R_L}{R_d}F_d$ (as $\frac{R_L}{R_d} \ll 1$), but the non-linearity corrections are taken into account according to Eq. (5) by using the measured values for $\frac{\partial^2 I}{\partial V^2}$ and $S(I)$.

In our measurement setup, bias-tees are used to separate dc bias and the bias-dependent noise signal at microwave frequencies. We use a liquid-helium-cooled low-noise amplifier (LNA) [17] with operating frequency range of $f = 600 - 950$ MHz. The noise signal is band limited to 600 - 850 MHz in order to avoid pick-up from mobile phones working at 940 MHz despite of a Faraday cage. After amplification of 80 dB, the signal was detected by a zero-bias Schottky diode with 0.5 mV/μW. A microwave switch and a tunnel junction were used to calibrate the gain. For more details we refer to Ref. 18.

Noise was measured using three different methods (in the order of increasing sensitivity): 1) noise at DC current 2) LOCK-IN detection of noise using sine-wave modulation of current, $I = I_{DC} + \delta I \sin(\omega t)$ where $I_{DC} \gg \delta I$, 3) current modulation by square-wave $\Pi(t)$, $I = I_{DC} + I_m \Pi(t/t_0)$ where $I_{DC} = I_m/2$. The calibration constants for each scheme were measured making similar experiments on a tunnel junction sample of a resistance of $R_T = 22$ kΩ. The data reported in this paper are mostly measured using method 2. Data obtained using method 3 agreed well with those measured with method 2, but the implementation of the non-linearity corrections turned out to be more problematic for method 3 than for 2. In addition to the above measurement schemes, we also performed experiments along method 2 where the DC bias was kept at zero and the noise modulation was measured at frequency 2ω while having the excitation at ω. By extrapolating the results of this method to $\delta I = 0$, we obtain the "zero-bias" Fano-factor. In the corrections using Eq. (5), we have estimated $i_n^2 = 2.5 \cdot 10^{-24}$ A^2 which is obtained from the noise temperature $T_N = 3.5$ K of our cooled LNA [17] using $i_n^2 = 4k_B T_N/R_L$ for the unmatched case, as $4k_B T_N/R_L$ is much larger than the shot noise generator $S_i = \widetilde{F} \cdot 2eI$.

Our nanotube sample was made using surface CVD growth with Fe catalyst. The length was $L = 0.7$ μm and the diameter $\phi = 2$ nm. The contacts on the nanotube were made using standard e-beam overlay lithography. In the contacts, 10 nm of Ti was employed as a sticking layer before depositing 70 nm of Al, followed by 5 nm of Ti. The width of the two contacts was 200 nm and the separation between the them was 0.3 μm. The electrically conducting body of the silicon substrate was employed as a back gate, separated from the sample by 100 nm of SiO_2.

A scan of differential conductance $G_d = \frac{dI}{dV}$ is displayed in Fig. 1. Clear maxima/minima in G_d with gate modulation are observed at zero bias, but no characteristic features of odd/even effects that are found in the Kondo regime of carbon nanotubes [19]. Therefore, we conclude that the pattern is due to Fabry-Perot (FP) interference even though it appears more asymmetrically-striped than observed typically [13, 14]. The maximum G_d is only about $1.0 \cdot G_0$ ($= 2e^2/h$) which indicates a rather weak coupling to one of the orbital modes of our nanotube sample (this will become more evident when discussing the shot noise data below). The contrast of the fringes, more than 100%, is clearly stronger than 10% - 30% found in Ref. 14. This may be connected with the fact that in our sample we are dealing mostly with interference within one mode.

To reach the Fabry-Perot regime, the quality of contacts has to be good [14]. This was investigated by making a separate cool down to 60 mK. No obvious change was observed in the $G_d(V, V_g)$ pattern, indicating that "odd-even" Kondo features do not appear even at dilution refrigerator temperatures. In this 2nd cool down, strong proximity-induced supercurrent was observed in the nanotube, which is another indication that the quality of the contacts is sufficient for the Fabry-Perot resonances. Furthermore, in our third cool-down, we were able to observe Kondo-type features. Such a change in the contacts is understandable as cool-downs are known to produce strain that may alter the contact configuration by a tiny amount.

Shot noise data (excess noise $S(I) - S(0)$) using small voltage bias $V = 0.1 - 10$ mV at $V_g = 0.04$ V are displayed in Fig. 2. The data can be fitted using an apparent power law $(S(I) - S(0)) \propto V^\beta$ with $\beta = 1.7$. This is clearly larger than the exponent $\beta = 0.64$ found in Ref. 12 at $V = 0.1 - 10$ mV, also at 4.2 K. In Fig.

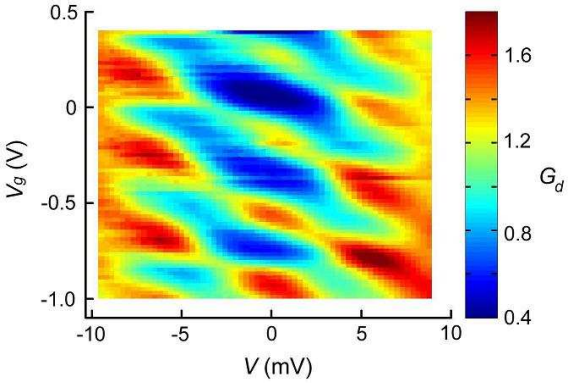

FIG. 1: (Color online) Differential conductance G_d on the plane spanned by bias voltage V and gate voltage V_g. The scale bar is given on the right in units of e^2/h ($= G_0/2$).

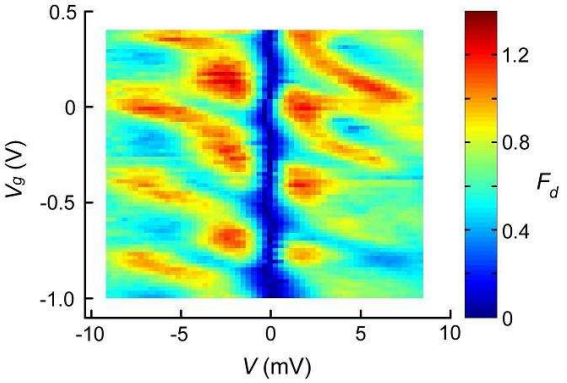

FIG. 3: (color online) Differential Fano-factor F_d on V_g vs. V plane. The scale bar is given on the right.

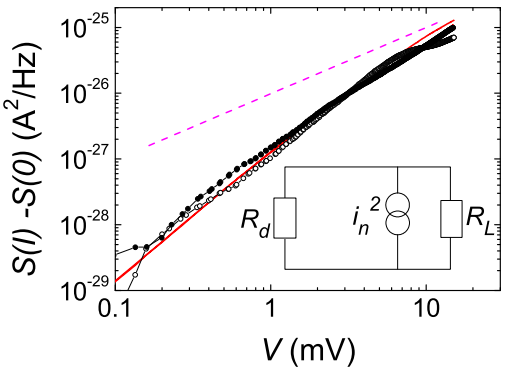

FIG. 2: Excess noise $S(I) - S(0)$ as a function of bias voltage $V > 0$ (○) and $V < 0$ (●). Red curve illustrates an evaluation of Eq. (4) using $F = 0.65$ and the experimentally determined value $R(0)/(V/I)$. The dashed line refers to exponent $\beta = 1$. The inset displays the electrical equivalent model employed to calculate the coupling of the current fluctuations as well as the corrections due to non-linearities.

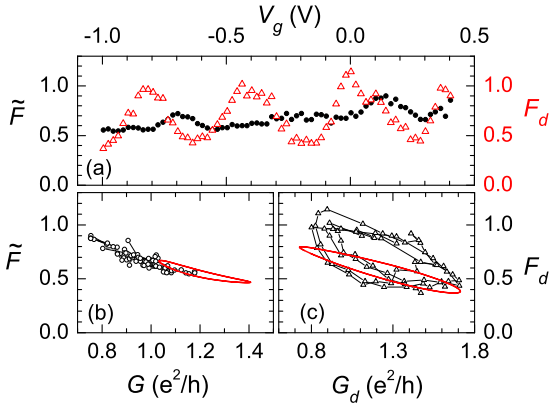

FIG. 4: Plots obtained using data of Figs. 1 and 3 at $V = -6.2$ mV. (a): Average differential Fano-factor $\widetilde{F} = \frac{1}{I}\int_0^I F_d dI$ (●) and differential Fano-factor $F_d = \frac{1}{2e}\frac{dS}{dI}$ (△) as a function of V_g. (b): $\widetilde{F}$ vs. total conductance $G = I/V$ plotted parametrically by varying V_g. (c): F_d vs. G_d plotted parametrically by varying V_g. For the overlayed curves, see text.

2, our data are compared with the cross-over formula of Eq. (4) using a Fano-factor $F = 0.65$, together with the experimentally measured (voltage-dependent) ratio for K. The measured Fano-factor is not exactly constant but, nevertheless, there is a good agreement between the measured data and Eq. (4). Thus, we have to conclude that Luttinger liquid behavior is not necessary to explain the power law dependence in our data.

The measured data on differential Fano-factor are displayed in Fig. 3. The picture reflects, more or less, the pattern of G_d in Fig. 1: ridges of large (small) F_d follow the ridges of small (large) G_d as would be expected for non-interacting, one mode conductor. The swing of F_d, however, exceeds 1, which is the upper limit in Landauer-Buttiker type of formalism for quantum dots and quantum point contacts [20]. At zero bias, F_d appears to go to zero, which is an artefact due to the employed AC-modulation scheme (method 2). At $V_g = 0$, we checked the low bias Fano by measuring noise at 2ω and varied the AC-modulation without any DC component. We obtained $F = 0.6 \pm 0.2$ as the modulation $\delta I \to 0$, which coincides with a smooth continuation of the data in Fig. 3. Basically, the ridges and gorges in Fig. 3 continue, with small modulation, all the way down to zero bias.

In Fig. 4, we interrelate the measured noise and conductance from Figs. 1 and 3 as suggested by Eqs. (1) and (3). At $V = -6.2$ mV in Fig. 4a, $\widetilde{F}$ does not display any oscillations as a function of gate voltage, only gradual large scale variation. The relation between $\widetilde{F}$ and $G = I/V$, displayed in Fig. 4b, appears linear. At other bias values, this dependence is similar to that of the differential quantities displayed in Fig. 4c. The linear relation between $\widetilde{F}$ and $G = I/V$ can qualitatively be

explained using non-interacting electron theory [21]. For F_d, however, such an analysis does not work. The dependence of F_d and G_d on V_g is found oscillatory with a small relative phase shift, which leads to ellipses in parametrically plotted curves of $F_d(V_g)$ *vs.* $G_d(V_g)$ in Fig. 4c. At $V > 0$, the relations between noise and conductance are similar, including unchanged rotation direction in the parametrically plotted ellipses.

Clearly, in the presence of two modes and interactions, no unique solution can be obtained for the transmission modes from the measurements of G_d and F_d. We have made a comparison with a phenomenological theory, assuming two modes with transmission coefficients of the form

$$\tau_i(\epsilon, V_g) = \overline{\tau}_i + m_i \cos\left[V_g/\Delta V_g \pm \epsilon/(e\Delta V) + \varphi_i\right], \quad (6)$$

where $i = 1$ or 2 is the number of the mode, $\overline{\tau}_i$ denotes the average value of their transmission, m_i gives the modulation depth of τ_i, and $\varphi_1 - \varphi_2$ specifies the relative phase difference of the transmission modulation. This form is taken as the basis of the Fabry-Perot resonances, which produce modulation of transmission coefficients along V_g and V-axes with periods ΔV_g and ΔV, respectively. The curve in Fig. 4 illustrates the result of a calculation for $\widetilde{F}$ and F_d using Eqs. (2) and (3) with parameters: $\overline{\tau}_1 = 0.48$, $\overline{\tau}_2 = 0.13$, $\varphi_1 - \varphi_2 = 0$, and $m_i = 0.5\overline{\tau}_i$ [22]. The model accounts for the main features of our data. It reproduces qualitatively deformed ellipses in parametric plots of $F(V_g)$ and $F_d(V_g)$ *vs.* $G_d(V_g)$, and the elongated shape (even with zero width) tracks the variation found in the experiments. According to the model, $\overline{\tau}_1$ dominates over $\overline{\tau}_2$ by a factor of $3 - 4$. This agrees with the previous discussion that a description of our data using a single dominant mode is a rather sound approximation.

In Ref. 23, lifting of mode degeneracies, both spin and orbital, was observed as the conductance was quantized in units of e^2/h. The asymmetry of the transport coefficient is so large in our sample that there might almost be a lifting of orbital degeneracy. However, since the asymmetry between $\overline{\tau}_1$ and $\overline{\tau}_2$ became smaller in subsequent cool-downs, we believe that the asymmetry comes rather from the details of the contact configuration not from actual removal of degeneracy. Thermally induced tension is a prime candidate for such deformations [24]. Moreover, there are first principles calculations using realistic contact structures which have yielded transport coefficients summing up to total conductance around 1 G_0, both for Ti and Al contacts [25], nicely in agreement with our conductance results.

In summary, using conductance and shot noise measurements, we have obtained evidence for quite asymmetric Fabry-Perot resonances in SWNTs. The Fano as well as the differential Fano-factor, ranging between 0.4 - 0.9 and 0.4 - 1.2, respectively, were found to depend on conductance either in linear or oscillatory fashion. We are able to explain our findings using a phenomenological model with two (spin-degenerate) modes having oscillatory, energy-dependent transmission coefficients of unequal magnitude. The large observed values of F_d, however, point towards the importance of interaction effects, which should be elaborated on theoretically in order to reach a full understanding of our results.

We wish to acknowledge fruitful discussions with S. Andresen, M. Buttiker, G. Cuniberti, R. Danneau, C. Glattli, F. Hekking, T. Heikkilä, T. Kontos, L. Lechner, B. Placais, and P. Virtanen. This work was supported by the TULE programme of the Academy of Finland and by the EU contract FP6-IST-021285-2.

[1] Ya. M. Blanter, M. Büttiker, Phys. Rep. **336**, 1 (2000).
[2] L. Saminadayar, D. C. Glattli, Y. Jin and B. Etienne, Phys. Rev. Lett. **79**, 2526 (1997).
[3] R. de-Picciotto, M. Reznikov, M. Heiblum, V. Umansky, G. Bunin, and D. Mahalu, Nature (London) **389**, 162 (1997).
[4] M. Henny, S. Oberholzer, C. Strunk, T. Heinzel, K. Ensslin, M. Holland, and C. Schönenberger, Science **284**, 296 (1999).
[5] W. D. Oliver, J. Kim, R.C. Liu, Y. Yamamoto, Science **284**, 299 (1999).
[6] C. L. Kane and M. P. A. Fischer, Phys. Rev. Lett. **72**, 724 (1994).
[7] P. E. Roche, M. Kociak, S. Gueron, A. Kasumov, B. Reulet, and H. Bouchiat, Eur. Phys. J. B **28**, 217 (2002).
[8] K. V. Pham, F. Piechon, K. I. Imura, and P. Lederer, Phys. Rev. B **68**, 205110 (2003).
[9] B. Trauzettel, I. Safi, F. Dolcini, and H. Grabert, Phys. Rev. Lett. **92**, 226405 (2004).
[10] E. Onac, F. Balestro, B. Trauzettel, C. F. J. Lodewijk, and L. P. Kouwenhoven, Phys. Rev. Lett. **96**, 026803 (2006).
[11] P. Recher, N. Y. Kim, Y. Yamamoto, cond-mat/0604613.
[12] N. Y. Kim, P. Recher, W. D. Oliver, Y. Yamamoto, J. Kong, H. Dai, cond-mat/0610196.
[13] T. Kontos, *et al.*, to be published.
[14] W. Liang, M. Bockrath, D. Bozovic, J. H.Hafner, M. Tinkham, and H. Park, Nature, **411**, 665 (2001).
[15] C. S. Peça and L. Balents, K. J. Wiese, Phys. Rev. B **68**, 205423 (2003).
[16] H. Birk, M. J. M. de Jong, and C. Schönenberger, Phys. Rev. Lett. **75**, 1610 (1995).
[17] L. Roschier and P. Hakonen, Cryogenics **44**, 783 (2004).
[18] F. Wu, L. Roschier, T. Tsuneta, M. Paalanen, T. Wang, and P. Hakonen, Conference Proceedings of "24th International Conference on Low Temperature Physics: LT24", Y. Takano, S. P. Hershfield, S. O. Hill, P. J. Hirschfeld, and A. M. Goldman, eds., (AIP Conference Proceedings **850**, ISBN 0-7354-0347-3) pp 1482-1483.
[19] See, J. Nygård, D. H. Cobden, and P. E. Lindelof, Nature **408**, 342 (2000), and references therein.
[20] But already taking in to account potential fluctuations due to charging and decharging can give $F > 1$, at least when the IV-curve is hysteretic. See, e.g., Ya. M. Blanter and M. Buttiker, Phys. Rev. B **59**, 10217 (1999).

[21] We have modelled the noninteracting transport as a sum of two modes with transmission coefficients τ_1 and τ_2 and evaluated the Fano-factor by setting $\tau_2 = 0.2$ and letting the other mode to account for the change in G: $\tau_1 = (G - \tau_2 * G_0)/(G_0)$. The small contribution of the second mode, $\tau_2 \sim 0.2$, is needed to lift $F(G)$ above the single mode curve $F = 1 - G/G_0$.

[22] The symmetry properties of $G(V, V_g)$ fix $\varphi_1 - \varphi_2 \sim 0$, the average G_d sets the sum $\overline{\tau}_1 + \overline{\tau}_2$, while the modulation of $G(V, V_g)$ ridges determines $\overline{\tau}_1/\overline{\tau}_2$. The modulation depth of τ_i was taken the same for both modes, yielding the optimum at 50%.

[23] M. J. Biercuk, N. Mason, J. Martin, A. Yacoby, and C. M. Marcus, Phys. Rev. Lett. **94**, 026801 (2005).

[24] Strain alone cannot lift the degeneracy of the bands, see, *e.g.*, E. D. Minot, Ph.D. thesis (Cornell University, 2004).

[25] J. J. Palacios, A. J. Perez-Jimenez, E. Louis, E. San-Fabian, and J. A. Verges, Phys. Rev. Lett. **90**, 106801 (2003).